1-1-2014

Experimental Validation Of A Robust Surge Speed Controller For Marine Surface Vessels

John Foehr
Wayne State University,

EXPERIMENTAL VALIDATION OF A ROBUST SURGE SPEED CONTROLLER FOR MARINE SURFACE VESSELS

by

JOHN V. FOEHR

THESIS

Submitted to the Graduate School

of Wayne State University,

Detroit, Michigan

in partial fulfillment of the requirements

for the degree of

MASTER OF SCIENCE

2014

MAJOR: MECHANICAL ENGINEERING

Approved by:

_____

Advisor Date

DEDICATION

To my mother, Marian.

ACKNOWLEDGEMENTS

I want to deeply and sincerely thank my advisor, Dr. Nabil Chalhoub for his guidance and direction. He is a true mentor, educator, and example. I am also thankful for my labmates Manan Trivedi and Costy Mastory, who provided instrumental help with this project.

TABLE OF CONTENTS

LIST OF FIGURES

NOMENCLATURE

$\hat{b}(x)$	=	Approximation of system parameters
$\hat{b}_r(\theta)$	=	Approximation of system parameters
η_r	=	Controller parameter determining speed of reaching the surface
η_s	=	Controller parameter determining speed of reaching the surface
F_r	=	Upper bound on the modeling imprecision
F_s	=	Upper bound on the modeling imprecision
$\hat{f}(x)$	=	A nominal function used to describe inertial effects along with all other resistive forces that may be applied on the vessel
$\hat{f}_r(\dot{\theta},\theta)$	=	A nominal function used to describe inertial effects along with all other resistive forces that may be applied on the arm
GPS	=	Global Positioning System
k_r	=	Controller gain
k_s	=	Controller gain
λ_r	=	Controller parameter determining sliding speed on the surface
λ_s	=	Controller parameter determining sliding speed on the surface
MSV	=	Marine Surface Vessel
ϕ_s	=	Parameter describing width of boundary layer
$s_r(\dot{\tilde{x}}_r,\tilde{x}_r)$	=	Sliding surface

$s_s\left(\dot{\tilde{x}}, \tilde{x}\right)$	=	Sliding surface
θ	=	Angular displacement of the throttle arm
v_c	=	Control voltage to the DC servomotor to rotate the throttle arm
$v_{c_{eq}}$	=	Equivalent control voltage
(X_i, Y_i)	=	i^{th} waypoint of the desired path
$\overline{x}_i$	=	Boat position projected onto the i^{th} segment of the desired path
$\dot{\overline{x}}_{i_c}^d$	=	Desired cruising speed
$\dot{\overline{x}}_{i_m}^d$	=	Desired maneuvering speed
$(\,)_s, (\,)_r$	=	Subscripts s and r correspond to surge speed controller and surge recovery controller, respectively

CHAPTER 1 INTRODUCTION

The current study centers around the experimental validation of the robust performance of a surge speed controller for autonomous piloting of under-actuated marine surface vessels. The controller design assumes no prior knowledge of the vessel's dynamics. In addition, all tests were conducted in open water under unpredictable and widely varying environmental conditions.

1.1 Motivation and Objectives

The overwhelming majority of marine surface vessels are under-actuated systems whereby the number of actuators is less than the number of degrees of freedom that need to be controlled. For trajectory tracking, marine surface vessels commonly utilize two actuators, namely, the propeller and the rudder, to control the surge speed, the sway motion, and the heading angle of the ship. The propeller thrust is employed for controlling the surge speed while the rudder action is used to simultaneously control the sway motion and the heading angle. This is usually performed by integrating the controller with a guidance system.

Due to the highly nonlinear behavior of marine surface vessels (Bulian, 2005; Nayfeh et al., 1973, 1974; Nayfeh and Mook, 1979; Sagatun and Fossen, 1991; Sagatun, 1992; Fossen, 1994; Suleiman, 2000; Vassalos, 1999; Vassalos et al., 2000; Lewandowski, 2004; Perez, 2005), accurate modeling of these systems for precision control is insurmountably difficult. Exemplary nonlinearities include coriolis and centripetal accelerations, wave excitation, nonlinear restoring forces, retardation forces, wind and sea-current resistive loads (Fossen, 1994; Lewandowski, 2004; Perez, 2005; Khaled and Chalhoub, 2011; Ogilvie, 1974; Ogilvie, 1983; Wang, 1976; Lee and

Newman, 1991; Fossen, 1994; Clamond et al, 2005). Therefore, the control challenges of under-actuated marine surface vessels are compounded by the facts that the dynamics of the vessel are not exactly known and the ship has to operate in a constantly varying environment, which is capable of producing unpredictable and considerable environmental disturbances induced by waves, wind, sea currents (Fossen, 1994; Perez, 2005), and ice floes (Cammaert and Muggeridge, 1988; Grace and Ibrahim, 2008).

Many recent studies have implemented advanced control algorithms on dynamic positioning, roll stabilization, heading, and tracking problems (Fossen, 1993; Fossen and Grovlen, 1998; Fossen, 2000; Moreira et al., 2007; Berge et al., 1998; Pivano et al., 2007; Godhavn, 1996; Strand et al., 1998; Pettersen and Nijmeijer, 2001; Fossen and Strand, 1999; Li et al., 2009; Aranda et al., 2002; Cimen and Banks, 2004; Lauvdal and Fossen, 1998; Do et al., 2003; Godhavn et al., 1998). However, the literature still lacks experimental validation of these controllers under realistic and mild to severe sea states. Therefore, the objective of the current work is to provide experimental validation for a modified version of a robust controller, proposed by Chalhoub and Khaled (2014), to control the surge speed of a marine surface vessel under realistic open-water conditions.

1.2 Literature Survey

Efforts to solve the challenging control problem of marine vessels date back to the early 1900s. In fact, the first implementation of the Proportional-Integral-Derivative (PID) controller can be found in a paper concerning ship auto-piloting for the United States Navy (Minorsky, 1922). PID controllers have, thenceforth, been used extensively in ship navigation systems due to their ease of use and implementation (Vahedipour and Bobis, 1992; Kallstrom et al., 1979; Vukic and Milinovic, 1996; Fossen, 1999; Moreira et

al., 2007; Francisco et al., 2008; Minghui, 2008). PID controllers are suitable for trajectory tracking in calm sea conditions, but during mild to severe weather conditions or intense maneuvering, the PID controllers become less reliable due to their inability to compensate for powerful disturbances and strong system's nonlinearities and uncertainties (Kallstrom et al., 1979). Around the same time as Minorsky (1922), Sperry mass produced and introduced gyrocompasses onto many marine vessels (Bennett, 1984). The use of gyrocompasses in marine vessels allowed for relatively accurate heading measurements for the first time. With Minorsky and Sperry's contributions, significant advances in the field of marine control have been realized, and PID controllers led the way (Minorsky, 1922; Bennett, 1984; Xiao and Austin, 2001; Moradi and Katebi, 2002; Caccia et al., 2008). PID controllers still account for over half of all controllers in the maritime industry (Ogata, 1997).

One of the main pursuits of this field is for marine vessels to achieve accurate tracking of predetermined desired trajectories via a guidance system paired with a control algorithm. Integrating the guidance system with the controller yields another layer of insurance that the vessel will remain on course. However, the most difficult control issue for marine vessels remains sea conditions, modeling imprecision, and the inherent system's nonlinearity, which have been proven to be challenging for PID controllers.

To alleviate the shortcomings of PID controllers, their gains have been varied with ship speed (Kallstrom et al, 1979). A direct comparison of a PID controller to a sliding mode controller, both modeled in an identical set up, shows better tracking performance and reaching speed across the board for the sliding mode controller (Perera and Guedes Soares, 2012).

Furthermore, many studies have introduced model-based controllers to control marine surface vessels (Van Amerongen, 1975; Van Amerongen, 1984; Lopez and Rubio, 1992; Moreira et al., 2007; Godhavn, 1996; Fossen, 1993; Fossen, 2000; Fossen and Grovlen, 1998; Berge et al., 1998; Strand et al., 1998). Backstepping algorithms with feedback dominance, as opposed to the typical feedback linearization, have been implemented (Li, Sun, and Oh, 2009). Nonlinear backstepping is very similar to feedback linearization techniques, the most notable difference between the two is that instead of complete cancellation of nonlinearities as in feedback linearization, backstepping actually exploits the so-called "good" nonlinearities and dampens "bad" nonlinearities (Fossen and Strand, 1999). Nonlinear backstepping has been shown to offer improvements over traditional PID or PD controllers in ship course keeping (Witkowska and Śmierzchalski, 2009). As with many nonlinear control methods, backstepping has a weakness in that it still relies on modeling accuracy. Other methods suffering the same weakness include linear quadratic regulators and linear quadratic tracking compensators (Lopez and Rubio, 1992), as well as standard feedback linearization (Fossen, 1993; Pettersen and Nijmeijer, 2001).

While model-based controllers can yield fairly good results in digital simulations, one would expect a significant degradation in their performances when implemented on an actual marine vessel operating under real world conditions. This is due to the adverse effects of structured and unstructured uncertainties that are not accounted for in the controller design.

To deal with marine vessels' nonlinearities, many studies have implemented nonlinear control schemes that are still heavily dependent on knowing the system's

dynamics (Fossen and Grovlen, 1998; Fossen and Strand, 1999a; Godhavn, 1996; Pettersen and Nijmeijer, 2001; Moreira et al., 2007). While these controllers are capable of handling known system's nonlinearities; their designs remain vulnerable to modeling imprecision and external disturbances. Thus, a control algorithm that can provide robustness despite system's nonlinearities and imperfect system model knowledge became paramount. Such a robust controller, which has its roots in the variable structure systems theory (Utkin, 1981; Rundell et al, 1996; Drakunov, 1983), is the sliding mode controller (Slotine and Li, 1991; Bazzi and Chalhoub, 2005; Chalhoub et al, 2006; Chalhoub and Khaled, 2009; Chalhoub and Khaled, 2014; Perera and Guedes Soares, 2012; Cheng, 2007; Lantos and Márton, 2011). These controllers do not require the system's dynamics to be fully known and can handle external disturbances as long as the upper bounds of modeling imprecision and external disturbances are known. It should be mentioned that most of the literature regarding sliding mode control of marine vessels is predominantly simulation based (Li et al, 2009; Hao et al, 2013; Borhaug, 2011; Kim, 2000; Cheng, 2007; Moreira et al, 2007; Khaled and Chalhoub, 2013; Fossen, 2002; Breivik, 2003; Chalhoub and Khaled, 2009; Breivik, 2003; Fossen, 1993; Perera, 2012). These studies demonstrate the robustness of the sliding mode controller in the presence of environmental disturbances and modeling inaccuracies.

Recently, many research studies have focused on combining the advantages of the sliding mode methodology with those of the fuzzy logic approach. This was done by using fuzzy inference systems (FIS) to provide on-line tuning of the sliding mode controller (Chalhoub et al, 2006; Ha et al, 1999; Choi and Kim, 1997; Lee et al, 2001). While other studies have used a self-tuned Takagi-Sugeno fuzzy logic controller whose

tuning terms involve switching functions based on sliding surfaces (Khaled and Chalhoub, 2013; Khaled and Chalhoub, 2014; Shaocheng and Li, 2009; Shaocheng et al, 2009). The asymptotic stability of such controllers is proven by the Lyapunov stability theory.

While there exists much theoretical work with simulations involving the control and guidance of marine surface vessels (Chalhoub and Khaled, 2009; Khaled and Chalhoub, 2013; Khaled and Chalhoub, 2014; Breivik, 2003; Fossen, 1993; Perera and Guedes Soares, 2012), actual experimental work is scarce. This is confirmed in the sample table, provided by Fahimi and Van Kleeck (2012), concerning the experimental work on marine surface vessels, which reveals a lack for outdoor experimental studies.

Ashrafiuon et al (2008) implemented a sliding mode controller to perform trajectory tracking tasks on an under-actuated autonomous surface vessel. The objective of the control law was to make the mass center of the boat accurately track a desired trajectory. The experimental work was conducted on a small-scale experimental system with a length of 0.45 m in a 1.9 m by 2.6 m indoor pool. Such a controlled environment cannot be used to demonstrate the robustness of the controller against wind, sea-currents, and wave excitations. Moreover, the concept of using the x and y coordinates of the mass center as output signals without feeding back the boat's orientation may work under calm sea conditions with hardly any disturbances (Fahimi and Van Kleeck, 2013). This is due to the longitudinal hydrodynamic forces, which cause the boat heading to be inherently stable under small perturbations. However, under significant environmental disturbances and with the lack of feeding back the heading angle, the controller will be oblivious to the heading errors and cannot compensate for them. As a consequence, the boat may be

pointing backward while its mass center accurately follows the desired trajectory (Fahimi and Van Kleeck, 2013).

To alleviate this problem, Fahimi and Van Kleeck (2013) and Schoerling et al (2010) have used a sliding mode controller to perform a trajectory tracking of a so-called "controlled" point, which is different from the mass center of the vessel. In their experimental work, Fahimi and Van Kleeck (2013) conducted their tests on a small boat having a mass of 7.8 kg and a length of 0.8 m. The tests were performed in a large outdoor pond in William Hawrelak Park, Edmonton, Alberta. The travel distance of the boat during the maneuver was less than 25 m. The desired path for the unmanned marine vessel was a figure eight. The desired speed of the vessel upon entering the desired trajectory was specified to be 0.25 m/s. This speed was then gradually increased to 0.5 m/s in a 15 s period. It was found that in case of large initial tracking errors, the sliding mode control signals would saturate for an extended period of time, which can cause stability problems. Therefore, a waypoint PD controller was then employed to reduce the initial tracking errors to certain level below which the sliding mode controller is activated. The controller, incorporating system dynamics in its design, performed well for both a calm day and a windy day; thus, demonstrating the viability of the sliding mode controller (Fahimi and Van Kleeck, 2012). It should be stressed that all these studies have incorporated nominal models of the boat in their controller design.

Instead of using a "controlled" point to perform trajectory tracking of the boat, the current work follows the trend of enabling under-actuated marine surface vessels to accurately track their desired trajectories by integrating the boat controller with a

guidance system (Moreira et al, 2007; Khaled and Chalhoub, 2013). Such an approach is currently a very active research field.

1.3 Thesis Overview

The aim and main contribution of this project is to experimentally implement and validate the sliding mode controller, developed by Chalhoub and Khaled (2014), in controlling the surge speed of an under-actuated 16 ft tracker boat in a completely uncontrolled real-world setting of the open-water in Lake St. Clair, Michigan. Moreover, the goal is to prove that sliding mode controllers can be successfully implemented without accounting for the boat's dynamics in their design; thus, rendering them to be model-less controllers.

The experimental set-up, used in generating the experimental results, is described in detail in the next chapter. Subsequently, the surge speed controller is presented in Chapter 3. The experimental results are shown in Chapter 4. They focus on proving experimentally the robust performance of the sliding mode controller in accurately tracking the desired surge speed profile in spite of significant environmental disturbances that are induced by wave excitations, sea-currents, and winds. Chapter 5 summarizes the work, highlights the findings of this study, and proposes prospective research topics in this field.

CHAPTER 2 EXPERIMENTAL SETUP FOR THE SURGE SPEED CONTROLLER

To ensure that a marine surface vessel (MSV) adheres to its desired trajectory, its longitudinal (surge) and transverse (sway) motions along with its yaw angular displacement have to be accurately controlled. A typical MSV has only two actuators to control its three degrees of freedom; thus, resulting in an under-actuated system. This challenging control task is generally addressed by coupling the controller with a guidance system (Moreira et al, 2007; Healey and Marco, 1992; Fossen, 2002; Breivik, 2003; Khaled and Chalhoub, 2013).

The first actuator is the propeller, which generates the thrust needed to control the surge speed of the boat. While the second actuator is the rudder that produces the moment required for steering the vessel. To operate the boat in a fully autonomous manner, the controller has to be able to automatically vary the thrust of the propeller and the rudder angle. Therefore, the marine vessel has to be retrofitted with two separate mechanisms that yield the control of the propeller thrust and the rudder angle to the controller. Since the scope of this study is limited to the control of the surge speed then only the mechanism that was built for varying the propeller thrust will be discussed in this chapter.

2.1 Description of the Experimental Setup

The marine vessel used in this work consists of a 4.88 *m* Tracker boat (see Fig. 2-1). The throttle mechanism, shown in Fig. 2-2, has been designed and built in-house to enable the controller to automatically rotate the handle that yields the desired propeller thrust. The entire mechanism is mounted on an X-Y table (Velmex model AXY2506) in

order to allow for a precise positioning and alignment of the mechanism with the throttle arm. Each axis of the table has a 5.08 *cm* range. The movement along each axis is caused by manual rotation of a leadscrew with a fine pitch of 0.254 *cm* per revolution.

The drive in the throttle mechanism has been selected to be a compact DC servomotor (Faulhaber model No. 3564) with a 12 V requirement for its nominal operation. The latter was a key factor in the selection of this particular drive due to the limited battery power supply on the boat. Moreover, the motor speed is rated at 822 rad/sec (7850 rpm) with a stall torque of 291 *mN.m*, which is not sufficient to rotate the stiff throttle handle. Therefore, a planetary gearhead (Faulhaber Series 38/2) with a gear ratio of 415:1 was then used in conjunction with the motor to produce a large control torque that can easily rotate the throttle handle.

An optical encoder (Faulhaber model No. HEDS5500C), capable of emitting 100 pulses per revolution, was mounted on the motor shaft. The encoder along with the high gear ratio of the gearhead has allowed the angular displacement of the throttle arm to be measured with a resolution of 0.0008675 degree/pulse. The emitted pulses of the encoder were counted by 24-bit up/down counters that are housed in the dSPACE1005 module (see Fig. 2-3).

The motor shaft is connected to the throttle arm by a coupler, which is passed through two tapered bearings to allow for smooth rotation and resist any axial loading that may be exerted on the motor shaft (see Fig. 2-2). The arm, which is rigidly attached to the coupler at its lower end, is used to transmit the rotational motion of the gearhead shaft to the throttle handle through a fork-shaped element. The latter is allowed to rotate with respect to the arm in order to avoid any sticking or jamming between the arm and

the throttle handle that may be induced by their misalignment. The fork-shaped element is supported by a collared shaft that goes through two tapered bearings that are mounted back-to-back in the upper end of the arm. The assembled system, shown in Fig. 2-2, provides the surge controller with the capability of directly changing the throttle angle in order to generate the required propeller thrust.

Two types of controllers are used in this work. The first one is the "surge speed" controller and the second one is the "surge recovery" controller. At any given time during a boat maneuver, only one of these controllers is active. The surge recovery controller is automatically activated by a high level monitoring code in case of emergency, which can be triggered by either a push of a panic button or by having the throttle handle exceeding its allowable range of rotation. In case of emergency, the monitoring code will override the surge speed controller and activate the surge recovery controller whose main objective is to bring back the throttle handle to the zero-thrust position in a controlled manner. The main feedback signal to the surge recovery controller is the angular displacement of the throttle arm, which is provided by the optical encoder that is mounted on the motor shaft (see Fig. 2-3).

On the other hand, the feedback signals for the surge speed controller are the (X,Y) coordinates of the boat with respect to a reference frame whose orientation is determined from a gyro-compass system (Cloud Cap Technology, Crista IMU). The origin of the reference frame is considered to coincide with the initial position of the boat, which is provided by a Hemisphere V101 Compass Global Positioning System (GPS) receiver that runs on a 12 V battery pack. The GPS has a serial connection over which it can send a wide variety of data packages. For the purpose of our work, the BIN1 data

packet, including latitude, φ, in degrees north and longitude, λ, in degrees east, has been selected. The measured data is converted to Universal Transverse Mercator (UTM) coordinates by using the following set of equations that were adopted from Ref. (Kawase, 2012):

$$E = E_0 + k_0 A\left[\eta' + \sum_{j=1}^{3} \alpha_j cos(2j\xi')sinh(2j\eta')\right] \tag{2-1a}$$

$$N = N_0 + k_0 A\left[\xi' + \sum_{j=1}^{3} \alpha_j sin(2j\xi')cosh(2j\eta')\right] \tag{2-1b}$$

where E refers to the "Easting" or the X coordinate while N signifies "Northing" or the Y coordinate. By convention, E_0 is set to $500\ km$ in a UTM zone, N_0 is assigned a zero value in the northern hemisphere, and the scale factor k_0 is given a value of 0.9996. Moreover, by considering the inverse flattening factor of the earth to be $1/f = 298.257223563$ and the equatorial radius R to be $6378.137\ km$, the following intermediary variables and parameters are computed as follows

$$n = \frac{f}{2-f} \qquad A = \frac{R}{1+n}\left(1 + \frac{n^2}{4} + \frac{n^4}{64} + \ldots\right)$$

$$\alpha_1 = \frac{1}{2}n - \frac{2}{3}n^2 + \frac{5}{16}n^3 \qquad \alpha_2 = \frac{13}{48}n^2 - \frac{3}{5}n^3 \qquad \alpha_3 = \frac{61}{240}n^3$$

$$\beta_1 = \frac{1}{2}n - \frac{2}{3}n^2 + \frac{37}{96}n^3 \qquad \beta_2 = \frac{1}{48}n^2 + \frac{1}{15}n^3 \qquad \beta_3 = \frac{17}{480}n^3$$

$$\delta_1 = 2n - \frac{2}{3}n^2 - 2n^3 \qquad \delta_2 = \frac{7}{3}n^2 - \frac{8}{5}n^3 \qquad \delta_3 = \frac{56}{15}n^3$$

$$\tau = sinh\left[tanh^{-1}sin(\varphi) - \frac{2\sqrt{n}}{1+n}tanh^{-1}\left(\frac{2\sqrt{n}}{1+n}sin(\varphi)\right)\right]$$

$$\lambda_0 = Z_n \times 6^0 - 183^0 \qquad \xi' = tan^{-1}\left(\frac{\tau}{cos(\lambda - \lambda_0)}\right) \qquad \eta' = tanh^{-1}\left(\frac{sin(\lambda - \lambda_0)}{\sqrt{1+\tau^2}}\right)$$

where Z_n is the zone number, which was found to be 17T for the area where the experimental work was conducted.

It should be pointed out that the Easting and Northing measurements in this study have a resolution of $0.6\,m$ due to the receiver's Differential GPS (DGPS). The DGPS utilizes ground-based reference station signals which serve as survey markers to improve upon the accuracy of the GPS satellite signal.

2.2 Chapter Summary

The experimental setup used in controlling the surge speed of the marine surface vessel has been discussed in this chapter. Autonomous physical manipulation of the throttle arm has been achieved via the proposed throttle mechanism. The measured GPS signals are converted to Universal Transverse Mercator (UTM) coordinates and fed back to the surge speed controller, which is covered in detail in the next chapter.

Fig. 2-1 Marine surface vessel used in the experimental work

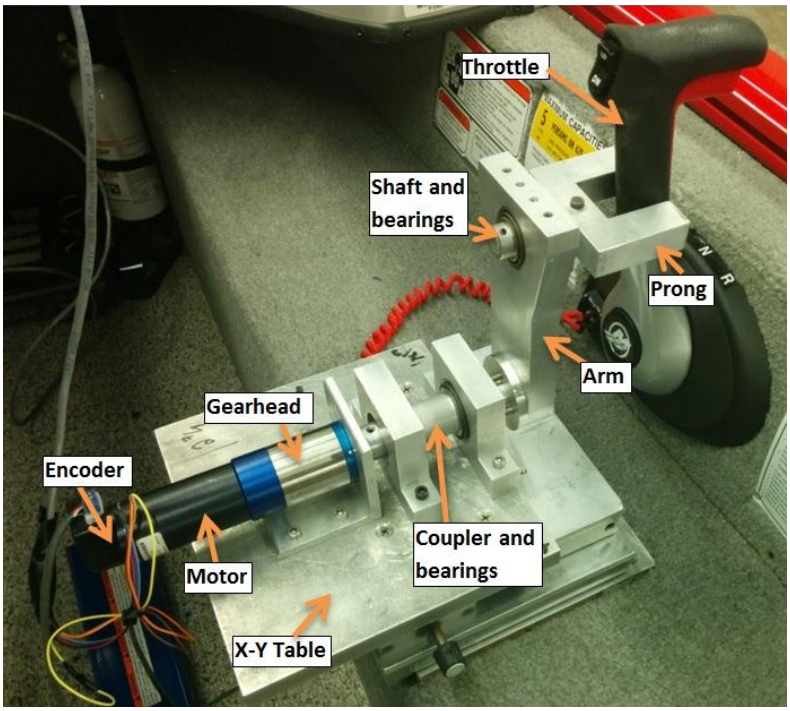

Fig. 2-2 Propeller thrust drive mechanism

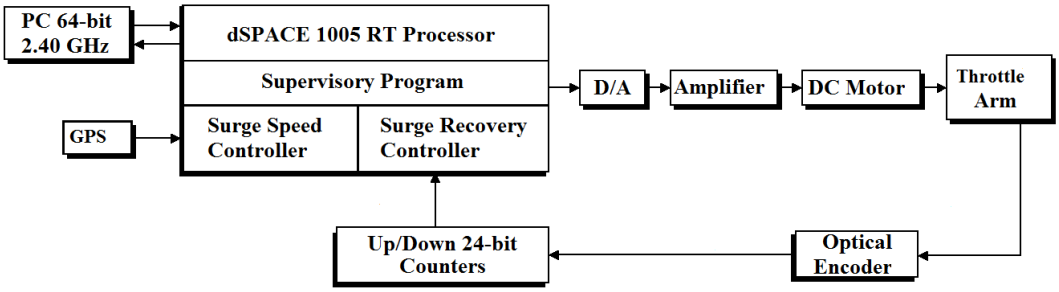

Fig. 2-3 Block diagram of the experimental set-up for controlling the surge speed

CHAPTER 3 DESIGN OF A SURGE SPEED CONTROLLER

The surge control problem of a marine surface vessel is a very challenging one due to the system's inherent nonlinearities and unpredictable environmental disturbances. To effectively deal with this tracking problem, a robust controller based on the slide mode methodology has been chosen in this work to cope with the modeling imprecision and external disturbances (Slotine and Li, 1991). Such controllers have been shown to exhibit robust performances in the presence of structured and unstructured uncertainties as long as the upper bounds on the modeling imprecision and external disturbances are known (Zhang, 2010; Hong, 1993; Cheng, 2007; Kim, 2000; Xu, 2005; Bazzi and Chalhoub, 2005; Chalhoub et al, 2006; Khaled and Chalhoub, 2011; Chalhoub and Matta, 2012).

Two robust nonlinear controllers were designed in this study. The objective of the first one is to perform the tracking task while the second one allows the boat to safely recover from an emergency situation. Both controllers along with their supervisory code will be described in detail in this chapter.

3.1 Hybrid Surge Speed Controller

A hybrid controller has been developed in this work to control the surge speed of a marine surface vessel. Its three main components are the supervisory code, the surge speed controller, and the recovery controller.

3.1.1 Supervisory Component

The supervisory component of the hybrid controller monitors the overall performance of the boat and decides whether the surge speed controller or the recovery controller should be activated. Currently, it has been developed to receive inputs from two different

sources. The first one is the signal from an emergency push button that can be pressed by a human observer based on his/her assessment of an impending dangerous situation. It should be stressed that this is the only human intervention that is allowed in the proposed fully autonomous operation of the marine vessel. Upon receiving such a signal, the supervisory code will abort the tracking task by deactivating the surge speed controller and enabling the recovery controller. The latter was designed in order to control the rate at which the boat speed is reduced down to zero. Note that an abrupt shut-off of the propeller thrust can jeopardize the safety of the crew and can cause a large rush of water to flood the stern of the boat.

The second source for triggering a switch from the surge speed controller to the recovery controller is the optical encoder that is mounted on the servo-motor shaft, which is used for rotating the throttle arm. During a boat maneuver, the supervisory code will continuously monitor the optical encoder signal representing the angular displacement of the throttle arm, $\theta(t)$. As long as $\theta(t)$ is within the specified range $[\theta_{\min}, \theta_{\max}]$, the supervisory code will keep the surge speed controller activated. Otherwise, it will switch to the recovery controller, which will send the throttle arm back to its initial position in a controlled manner. Note that $\theta_{\max}$ is specified to limit the maximum propeller thrust available during a given boat maneuver. This is done to safeguard against any unstable behavior of the closed-loop system. Furthermore, the current system can only provide positive values of the propeller thrust. Therefore, $\theta_{\min}$ has been set to prevent the controller from driving the throttle handle into the neutral or reverse position.

3.1.2 Surge Speed Controller

The objective of the surge speed controller is to track a speed profile specified along the desired trajectory of the marine surface vessel. The trajectory is usually defined by a set of waypoints connected by straight segments. Figure 3-1 illustrates the position of the vessel with respect to the i^{th} segment of the trajectory. The boat position is projected onto this segment to yield a local coordinate $\bar{x}_i$ defined along the direction of the segment and represents the location of the projection point with respect to the i^{th} waypoint (X_i, Y_i). The desired surge speed profile along any segment has been designed to have an acceleration phase, a cruising phase, and a deceleration phase.

For the purpose of illustration, a flattened multi-segment desired trajectory has been drawn in Fig. 3-2. The surge speeds at both initial and final waypoints have been set to zero. The circles of acceptance represent zones where the boat undergoes turning maneuvers during which the surge speed will be reduced from cruising speed, $\dot{\bar{x}}_{i_c}^d$ to maneuvering speed, $\dot{\bar{x}}_{i_m}^d$. In the first segment between (X_1, Y_1) and (X_2, Y_2) waypoints, the desired speed profile reveals a constant acceleration phase whereby the vessel speed is increased from 0 to a specified cruising speed, $\dot{\bar{x}}_{i_c}^d$. The latter is expected to vary with the sea-state. A cruising phase will follow and remains in effect till the boat reaches the circle of acceptance that is centered at (X_2, Y_2). At this point, a constant deceleration phase will begin till the vessel speed reaches $\dot{\bar{x}}_{i_m}^d$. The maneuvering speed is maintained until the boat exits the circle of acceptance at which point the acceleration phase for the

subsequent segment will begin. This pattern is repeated for all segments of the trajectory. The desired velocity profile is generated by a MATLAB code that yields the desired surge speed as a function of distance from the initial waypoint of the segment. Distance-dependent velocity profile along a segment is advantageous, particularly when the waypoints are selected close enough to each other to prevent the vessel from accelerating to the cruising speed and then decelerating to the maneuvering speed. Thus, in the event that the boat approaches the final waypoint of a segment before it has had the time to reach its cruising speed then the vessel will start decelerating to the maneuvering speed in order to make the turn safely. This scenario is illustrated in the speed profile of the third segment in Fig. 3-2, which clearly reveals the absence of a cruising phase. It should be pointed out that the acceleration and deceleration rates along with the cruising and maneuvering surge speeds are set to practical values based on the sea-state.

Next the surge speed controller is designed based on the sliding mode methodology. The controller is similar in concept to the one devised by Chalhoub and Khaled (2014) but slightly modified to make it suitable for the current experimental work. The objective of the current work is to experimentally validate the performance of the proposed surge speed controller in the presence of considerable modeling imprecision and environmental disturbances. The nominal state equation for the surge motion of the boat can be written as follows

$$\dot{x} = f(x) + b(x)v_c \tag{3-1}$$

where $x = \dot{\bar{x}}_i$ is the surge speed along the i^{th} segment of the trajectory. It is deduced from the measured data of the GPS. Moreover, $\hat{f}(x)$ is a nominal function used to describe inertial effects along with all other resistive forces that may be applied on the

vessel. v_c is the control voltage for the DC servomotor responsible for rotating the throttle arm. A ± 10V saturation limits were placed on the output control signal to prevent overloading the 12V servomotor. The $\hat{f}(x)$ and $\hat{b}(x)$ terms represent the best approximations available for the actual $f(x)$ and $b(x)$ functions, which will never be known with absolute certainty in a real life situation. $\hat{b}(x)$ is approximated as follows (Slotine and Li, 1991):

$$\hat{b} = \sqrt{b_{\min} b_{\max}} \tag{3-2a}$$

$$\beta = \sqrt{\frac{b_{\max}}{b_{\min}}} \tag{3-2b}$$

where $b_{\min}$ and $b_{\max}$ are assumed to be known. An integral form of the sliding surface has been selected:

$$s_s\left(\dot{\tilde{x}}, \tilde{x}\right) = \left(\frac{d}{dt} + \lambda_s\right)^2 \int_0^t \tilde{x}\, d\tau \quad \text{where} \quad \tilde{x} = \int_0^t \left(\dot{\tilde{x}}_i - \dot{\tilde{x}}_i^d\right) d\tau \tag{3-3}$$

where λ_s is a control parameter. By setting $\dot{s}_s = 0$, one would get the equivalent control signal to be

$$\dot{s}_s = 0 \quad \Rightarrow \quad v_{c_{eq}} = \frac{1}{\hat{b}}\left[-\hat{f} + \ddot{\tilde{x}}_i^d - 2\lambda_s \dot{\tilde{x}} - \lambda_s^2 \tilde{x}\right] \tag{3-4}$$

The complete expression of the control signal is given by

$$v_c = v_{c_{eq}} - \frac{k_s}{\hat{b}} \operatorname{sgn}\left(s_s\right) \tag{3-5}$$

The gain k_s is determined by satisfying the following sliding condition:

$$\frac{1}{2}\frac{d\left(s_s^2\right)}{dt} \le -\eta_s \left|s_s\right| \tag{3-6}$$

where η_s is a control parameter. To satisfy the above inequality, k_s has to be:

$$k_s \geq \beta(\eta_s + F_s) + |\beta - 1|\left|\hat{f} + 2\lambda_s\dot{\tilde{x}} + \lambda_s^2\tilde{x} - \ddot{x}_i^d\right| \tag{3-7}$$

Note that F_s is the upper bound on the modeling imprecision. It is defined as

$$F_s \geq \left|f - \hat{f}\right|_{\sup} \tag{3-8}$$

In addition, the term β, defined in Eq. (3-2b), satisfy the following inequality (Slotine and Li, 1991):

$$\beta^{-1} \leq b^{-1}\hat{b} \leq \beta \tag{3-9}$$

To minimize the chattering in the control signal when the vessel is operating in the vicinity of the sliding surface, the $sgn(s_s)$ term has been substituted by a saturation function in Eq. (3-5) as follows

$$v_c = v_{c_{eq}} - \frac{k_s}{\hat{b}}\,\mathrm{sat}\left(\frac{s_s}{\phi_s}\right) \tag{3-10}$$

where the ϕ_s term represents the thickness of the boundary layer surrounding the sliding surface.

3.1.3 Recovery Controller

The objective of the recovery controller is to decrease the surge speed to zero in a controlled manner in order to avoid any abrupt change in the operating conditions of the boat. The inputs of the controller are the angular displacement, θ, and velocity, $\dot{\theta}$, of the throttle arm as measured by the optical encoder. The nominal equation of motion of the throttle arm including the dynamics of the actuator can be expressed in the following general form as

$$\ddot{\theta} = f_r(\dot{\theta}, \theta) + b_r(\theta)v_c \tag{3-11}$$

Note that $\dot{\theta}$ is deduced from the optical encoder measurement. v_c is the control voltage for the DC servomotor responsible for rotating the throttle arm. Both $\hat{f}_r\left(\dot{\theta},\theta\right)$ and $\hat{b}_r\left(\theta\right)$ are approximations of the actual $f_r\left(\dot{\theta},\theta\right)$ and $b_r\left(\theta\right)$, which are unknown functions. Similar to the design of the surge speed controller, $\hat{b}_r\left(\theta\right)$ is approximated as follows (Slotine and Li, 1991):

$$\hat{b}_r = \sqrt{b_{r_{\min}} b_{r_{\max}}} \tag{3-12a}$$

$$\beta_r = \sqrt{\frac{b_{r_{\max}}}{b_{r_{\min}}}} \tag{3-12b}$$

$$\beta_r^{-1} \le b_r^{-1}\hat{b}_r \le \beta_r \tag{3-12c}$$

The sliding mode recovery controller is considered to have the following sliding surface:

$$s_r\left(\dot{\tilde{x}}_r,\tilde{x}_r\right) = \dot{\tilde{x}}_r + \lambda_r\tilde{x}_r \quad \text{where} \quad \tilde{x}_r = \theta - \theta^* \tag{3-13}$$

where λ_r is a control parameter and θ^* is assigned an appropriate constant value. By setting $\dot{s}_r = 0$, the equivalent control signal becomes

$$v_{c_{eq}} = -\frac{1}{\hat{b}_r}\left[\hat{f}_r + \lambda_r\dot{\tilde{x}}_r\right] \tag{3-14}$$

The complete expression of the control signal is given by

$$v_c = v_{c_{eq}} - \frac{k_r}{\hat{b}_r}\operatorname{sgn}\left(s_r\right) \tag{3-15}$$

The gain k_r is determined by satisfying the following sliding condition:

$$\frac{1}{2}\frac{d\left(s_r^2\right)}{dt} \le -\eta_r\left|s_r\right| \tag{3-16}$$

where η_r is a control parameter. To satisfy the above inequality, k_r has to be:

$$k_r \geq \beta_r \left(\eta_r + F_r\right) + \left|\beta_r - 1\right| \left| \hat{f}_r + \lambda_r \dot{\tilde{x}}_r \right| \tag{3-17}$$

Note that F_r is the upper bound on the modeling imprecision. It is defined as

$$F_r \geq \left| f_r - \hat{f}_r \right|_{\sup} \tag{3-18}$$

Again, a saturation function was substituted for the "sgn" function in the control signal to yield:

$$v_c = v_{c_{eq}} - \frac{k_r}{\hat{b}_r} \text{sat}\left(\frac{s_r}{\phi_r}\right) \tag{3-19}$$

where the ϕ_r term represents the thickness of the boundary layer surrounding the sliding surface.

The surge speed and recovery controllers have been built in MATLAB Simulink and downloaded to a dSPACE 1005 Real-time processor for on-line implementation.

3.2 Summary

This chapter covers the design of the hybrid surge speed controller. Its three major components comprise of the supervisory code, the surge speed controller, and the recovery controller. These components have been discussed herein in great detail.

The hybrid surge speed controller is experimentally validated by the experimental work that will be described in the next chapter.

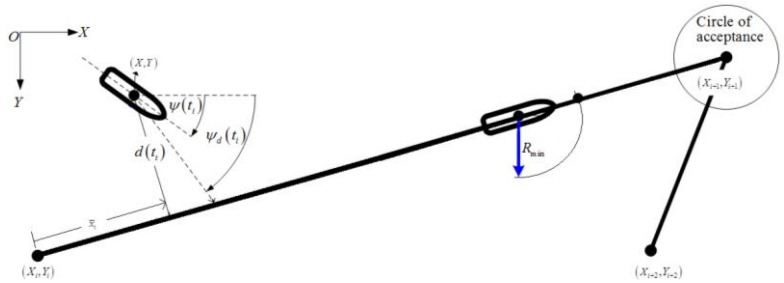

Fig. 3-1 Relative position of the vessel with respect to the i^{th} segment of its desired trajectory

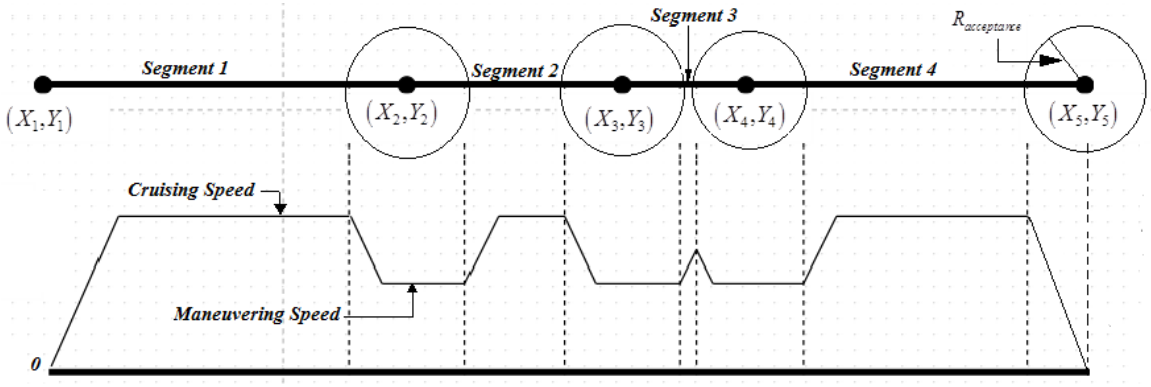

Fig. 3-2 Surge speed profile along a flattened multi-segment desired trajectory of the marine surface vessel

CHAPTER 4 EXPERIMENTAL VALIDATION OF THE SURGE SPEED CONTROLLER

Most of the work that has been reported in the literature pertaining to the robust and adaptive control of marine surface vessels has been limited to digital simulations (Chalhoub and Khaled, 2009; Khaled and Chalhoub, 2013; Khaled and Chalhoub, 2014; Breivik, 2003; Fossen, 1993; Perera and Guedes Soares, 2012). The few experimental studies in this field have implemented advanced control schemes on very small scale marine systems and the tests were carried out either in indoor pools/tanks (Ashrafiuon et al, 2008; Li et al, 2009) or in an outdoor pond (Fahimi and Van Kleeck, 2013; Schoerling et al, 2010). All these studies have dealt with hobby-type marine vessels. Therefore, there is an urgent need for experimental validation of the theoretical advances in control theory on actual marine surface vessels to be conducted in a completely uncontrolled real-life setting. It is the intent of this chapter to provide an experimental validation of the surge speed sliding mode controller proposed by Chalhoub and Khaled (2014).

4.1 Experimental Results

The experimental data were generated by using the modified 16 ft (4.88 *m*) tracker boat that was described in Chapter 2 (see Fig. 2-1). The throttle mechanism, shown in Fig. 4-1, has been designed to yield the control of the propeller thrust to the sliding mode controller. In any test, two types of controllers were implemented. The first one is the "sliding mode surge speed" controller while the second one is a "surge recovery" controller. At any given time during a boat maneuver, only one of these

controllers is active. The surge recovery controller is automatically activated by a high level monitoring code in case of emergency, which can be triggered by either

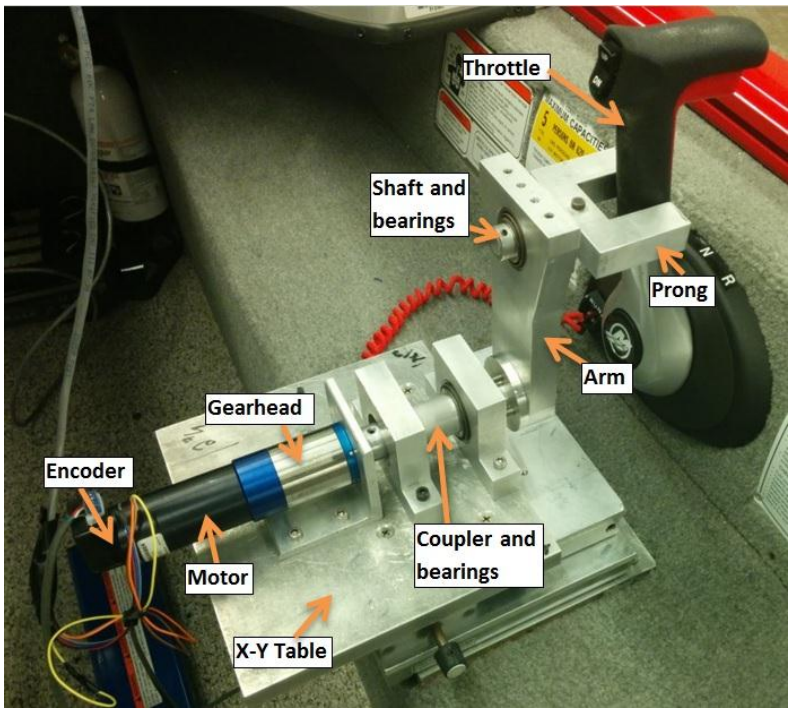

Fig. 4-1 Propeller thrust drive mechanism

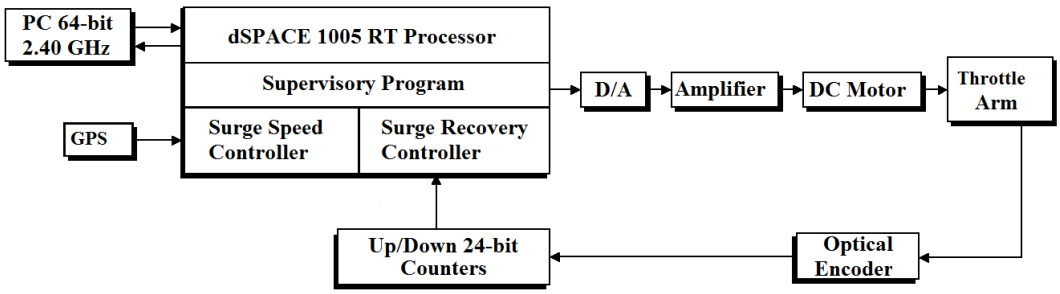

Fig. 4-2 Pictorial description of the surge speed controller

a push of a panic button or by having the throttle handle exceeding its allowable range of rotation. In case of emergency, the monitoring code will override the sliding mode surge speed controller and activate the surge recovery controller whose main objective is to bring the throttle handle back to the zero-thrust position in a controlled manner. This is pictorially depicted in Fig. 4-3, which reveals that the main feedback signal to the surge recovery controller is the angular displacement of the throttle arm, which is measured by the optical encoder that is mounted on the motor shaft. However, the feedback signals to the sliding mode surge speed controller are the (X,Y) coordinates of the boat with respect to a reference frame whose origin is considered to coincide with the initial position of the boat. The latter is provided by a Hemisphere V101 Compass Global Positioning System (GPS) receiver.

The desired surge speed profile is shown in Fig. 4-3 with respect to time. This profile corresponds to the desired surge speed along two straight line segments connecting three waypoints of a specified trajectory. It consists of ramping up the boat speed to 12 km/hr (3.333 m/s) in 5 seconds, cruising at 12 km/hr for 55 seconds, decelerating to 9 km/hr (2.5 m/s) in 15 seconds, cruising at the lower speed for 10 seconds, ramping up the speed back to 12 km/hr in 5 seconds, cruising at 12 km/hr for 52 seconds, and then decelerating for 20 seconds. The specified profile of Fig. 4-3 will require the boat to traverse a total distance of 444.4 m during this test (see Fig. 4-4), which caused the boat to endure significantly different wave heights and conditions in the rough environment of Lake St. Clair.

It should be pointed out that all tests were conducted without allowing negative propeller speed; thus, the controller can only reduce or bring down the propeller speed to

zero (no negative propeller thrust). This is the reason why the deceleration period was specified to be significantly longer than the acceleration period in the desired surge speed profile of Fig. 4-3.

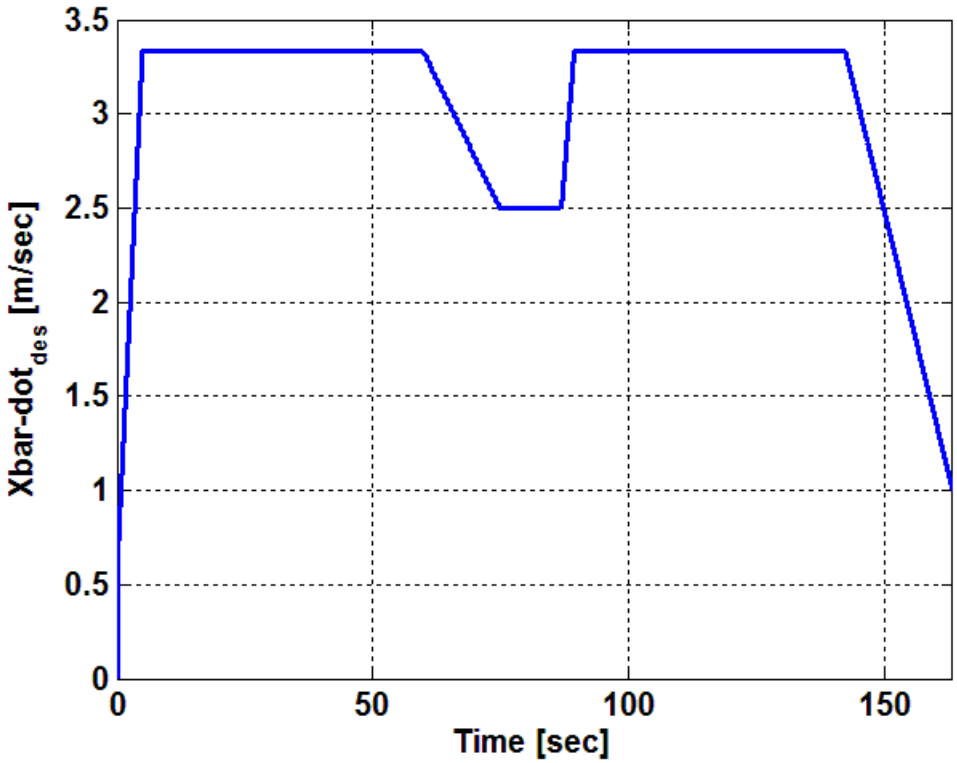

Fig. 4-3 Desired surge speed profile with respect to time

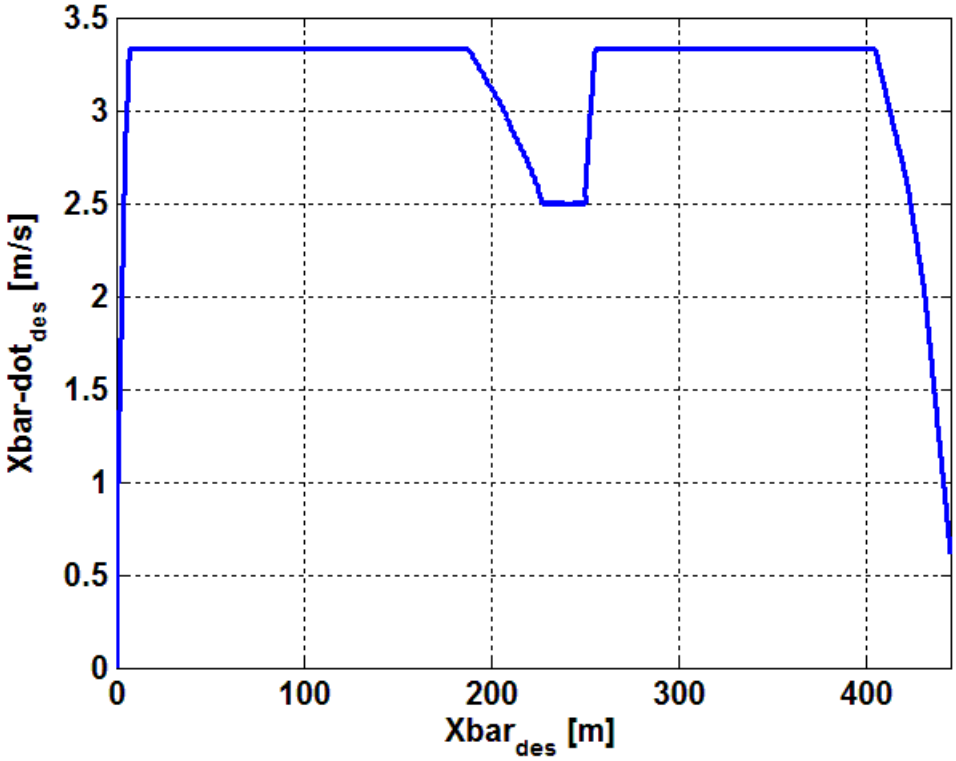

Fig. 4-4 Desired surge speed profile with respect to boat position

However, the profile in Fig. 4-3 is defined with respect to time. This can certainly be problematic, particularly, in cases where the boat might experience a severe resistance from waves, sea currents, or winds. Under such circumstances, the propulsion system may not be able to produce the thrust required to generate or maintain the desired surge speed. Consequently, the positional error of the boat may accumulate and the marine vessel may encounter situations whereby the boat is moving along the i^{th} segment of the trajectory while the reference signal given to the controller pertains to the $(i+1)^{th}$ segment. This difficulty has been circumvented in this work by specifying the desired surge speed profile as a function of the boat position along the desired trajectory. Thus, the desired surge speed profile of Fig. 4-4, instead of Fig. 4-3, was used in controlling the surge speed of the marine vessel.

The current experimental work aimed at validating the robust performance and good tracking characteristic of the sliding mode surge speed controller that was presented in Chapter 3. The test was conducted in the open-water of Lake St. Clair in Michigan. The wave height ranged from 1 to 2 ft. The experimental results are illustrated in Figs 4-5 to 4-8. Figure 4-5 serves to prove the good tracking characteristic of the controller in spite of significant wave excitations that varied considerably from one region in the lake to another. This is clearly manifested by the large fluctuations of the actual surge speed around the desired one during the second segment of the desired trajectory. These fluctuations were also present but to a much lesser extent as the boat traversed the first segment of the desired trajectory. These results serve to prove the robustness of the controller not only to environmental disturbances, induced by waves, wind, and sea currents, but also to the marine vessel dynamics, which were completely ignored in the

design of the controller. Note that the spikes in Fig. 4-5 stem from anomalies in the GPS raw data.

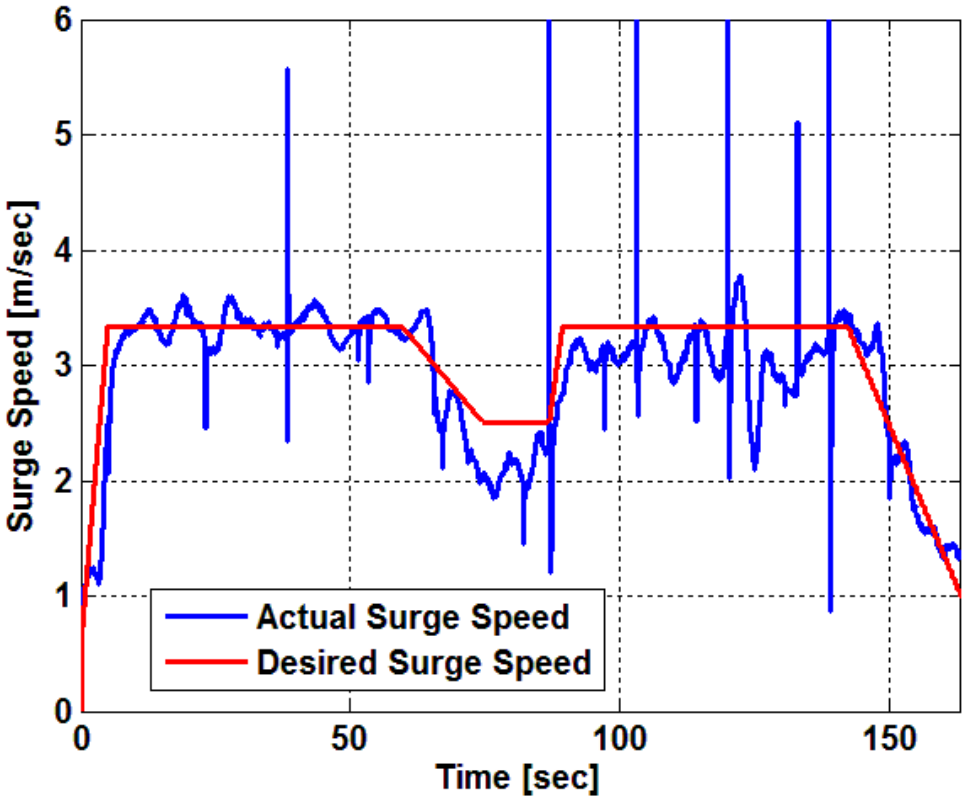

Fig. 4-5 Actual and desired surge speed of the marine vessel

Both the sliding surface, s_{surge}, and the control signal, u_{surge} are shown in Fig. 4-6. For good tracking, s_{surge} should be ideally kept at zero after the reaching phase. However, due to modeling imprecision and external disturbances, s_{surge} will deviate from zero. Therefore, the s_{surge} deviations from zero during the cruising phases are primarily induced by wave excitations and sea currents and to a lesser extent to wind. However, the controller was always able to converge s_{surge} to zero; thus, recovering from the environmental disturbances. It should also be noted that the large deviation of s_{surge} during the first few seconds is attributed to the reaching phase during which the system is recovering from a mismatch between the initial values of the actual and desired boat speeds. Furthermore, s_{surge} took large values during the deceleration phase. This is because negative propeller speeds were not allowed in the current work. As a consequence, the controller can only reduce or bring down the propeller speed to zero; thus, handicapping the capability of the controller in the deceleration phase. Therefore, a realistic desired deceleration profile cannot be specified to be faster than the rate at which the boat's momentum can die out to zero. This is the rationale behind specifying the deceleration phases to be three to four times longer than the acceleration phases.

Figure 4-6 reveals that the control signal is always dominated by the switching term due to the fact that u_{surge} is always out-of-phase with s_{surge}, which is one of the main characteristic of the sliding mode controller.

Moreover, the spikes in the curves of Fig. 4-6 reflect the sensitivity of both the sliding surface and the control signal to anomalies in the GPS raw data. Thus, ways for

removing these anomalies from the GPS data should be further investigated in order to remove their direct

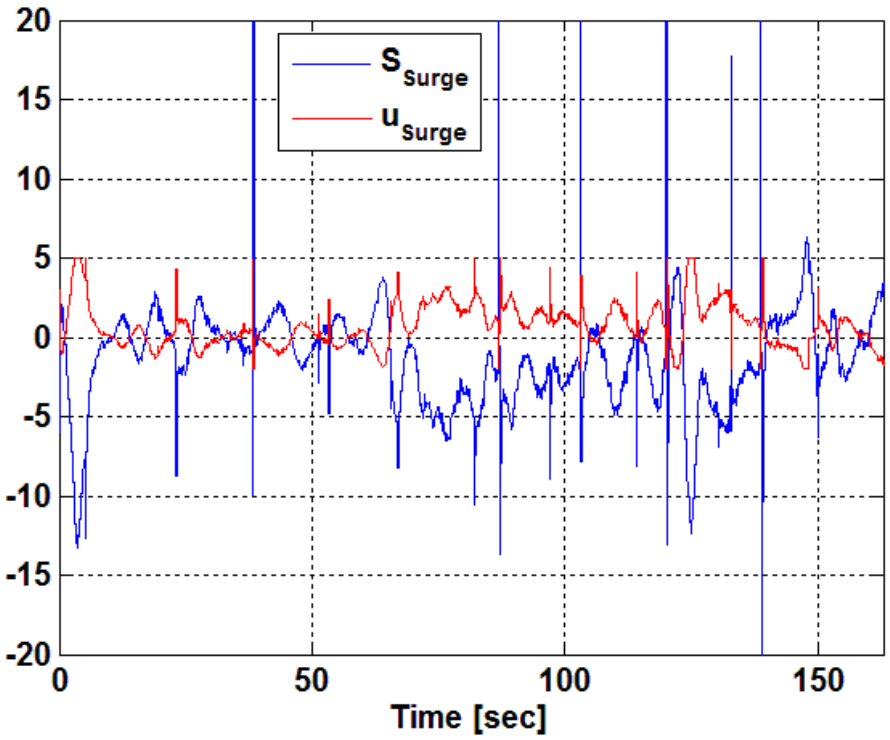

Fig. 4-6 Sliding surface and surge speed control signal

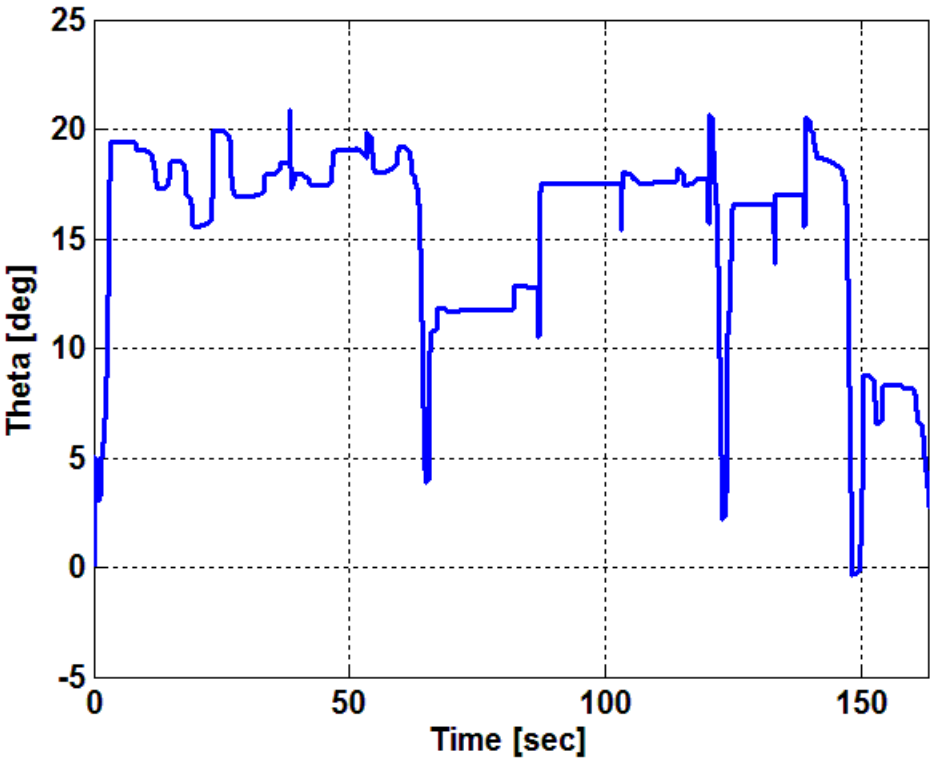

Fig. 4-7 Angular displacement of the control handle of the propeller thrust

adverse effects on the controller performance. Figure 4-7 reveals the angular displacement of the control handle of the propeller thrust.

4.2 Summary

The experimental setup described in Chapter 2 has been used to experimentally validate the sliding mode surge speed controller that was described in Chapter 3. The results served to demonstrate and experimentally validate the robustness and good tracking capability of the proposed surge speed controller in the presence of considerable and unpredictable environmental disturbances induced by wave excitations, sea-currents, and winds. Moreover, the good performance of the boat was achieved in spite of the fact that the controller completely ignored the dynamics of the marine vessel in its design; thus, proving the controller robustness to significant unstructured uncertainties.

CHAPTER 5 SUMMARY AND MAIN CONTRIBUTIONS

This chapter summarizes the work, highlights the findings of this study, and proposes prospective research topics in this field.

5.1 Goal of the Project

The present work centers around the experimental validation of the robust performance and good tracking characteristic of a sliding mode surge speed controller (Chalhoub and Khaled, 2014) for autonomous piloting of an under-actuated 16 ft tracker boat in a completely uncontrolled real-world setting of the open-water of Lake St. Clair, Michigan. Furthermore, the goal is to prove that sliding mode controllers can be successfully implemented to track the desired surge speed without considering the dynamics of the marine vessel in their design; thus, rendering them to be model-less robust controllers.

5.2 Summary

The overwhelming majority of marine surface vessels (MSV) are under-actuated systems. This is because a typical MSV has only the propeller and the rudder to control its surge, sway and yaw motions. The propeller generates the thrust needed to control the surge speed of the boat. While the rudder is used to simultaneously control the heading angle and the sway motion of the boat. Normally, this is done by coupling the controller with the guidance system.

To automate the surge speed control process, the controller has to be able to automatically vary the thrust of the propeller as needed. Therefore, the marine vessel has

been retrofitted with a new drive mechanism (see Fig. 2-2) that yields the control of the propeller thrust to the controller. The new drive mechanism has been designed and built in-house. Its detailed description is provided in Chapter 2.

The surge control problem is a very challenging one due to the system's inherent nonlinearities and unpredictable environmental disturbances. To effectively deal with this tracking problem, a robust controller based on the slide mode methodology has been chosen in this work to cope with the modeling imprecision and external disturbances (Chalhoub and Khaled, 2014). This type of controller has been shown to exhibit robust performances in the presence of structured and unstructured uncertainties as long as the upper bounds on the modeling imprecision and external disturbances are known.

To safely implement the controller on a marine vessel operating in the open-water of a real life setting such as Lake St. Clair, a hybrid controller has been developed in this work. It has three main components consisting of a supervisory algorithm, a surge speed controller, and a recovery controller. All controllers were designed based on the sliding mode methodology. At any given time during the operation of the boat, only one of the two controllers is activated. The surge recovery controller is automatically activated by a high level monitoring algorithm in case of emergency, which can be triggered by either a push of a panic button or by having the control handle of the throttle thrust exceeding its allowable range of rotation. In case of emergency, the monitoring code will override the surge speed controller and activate the surge recovery controller whose main objective is to bring back the throttle handle to the zero-thrust position in a controlled manner. The main feedback signal to the surge recovery controller is the angular displacement of the control handle. On the other hand, the feedback signals for the surge speed controller are

the (X,Y) coordinates of the boat with respect to a reference frame, which are provided by a Hemisphere V101 Compass Global Positioning System (GPS) receiver. Its objective is to track a surge speed profile specified along the desired trajectory of the marine surface vessel in spite of considerable modeling imprecision and environmental disturbances that are induced by waves, sea-currents, and wind. A typical profile for the desired surge speed is shown in Fig. 3-2. The details of both the surge speed controller and the recovery controller are covered in Chapter 3.

The majority of advanced control algorithms that have been developed for the control of marine surface vessels have only been tested in digital simulations. Very few studies have attempted to provide experimental results by employing hobby-type marine vessels. However, their experimental validation has been performed on very small scale marine systems and in controlled environments such as indoor pools/tanks or an outdoor pond.

In the current study, the proposed hybrid controller was used a 16 ft (4.88 *m*) tracker boat and all tests were conducted in a completely uncontrolled environment of Lake St. Clair in Michigan. The results served to demonstrate and experimentally validate the robustness and good tracking capability of the proposed control scheme in the presence of considerable and unpredictable environmental disturbances induced by wave excitations, sea-currents, and winds. Moreover, the good performance of the boat was achieved in spite of the fact that the controller completely ignored the dynamics of the marine vessel in its design; thus, proving the controller robustness to significant unstructured uncertainties.

5.3 Main Contributions of this Project

The main contributions are:

- Development of a hybrid surge speed controller entailing a supervisory code, a surge speed controller, and a recovery controller.
- Designed and built in-house a new drive mechanism which yields the control of the propeller thrust to the surge speed controller.
- Provide experimental validation of the robustness and the good tracking characteristic of the sliding mode surge speed controller in an uncontrolled real life setting with unpredictable and widely varying environmental conditions.

5.4 Prospective Research Topics

The following is a suggested list of future research topics in this field:

- Improve the performance of the surge speed controller by eliminating the anomalies in the GPS raw data.
- Expand the hybrid controller to include heading control and validate the system through experimental work.
- Couple the expanded version of the hybrid controller with a guidance system and validate the coupled system through experimental work.

REFERENCES

[1] Aranda, J., De La Cruz, J.M., Díaz, J.M., Dormido Canto, S., 2002, "qft versus classical gain scheduling: study for a fast ferry," 15th IFAC World Congress.

[2] Ashrafiuon, H., Muske, K.R., McNinch, L.C., Soltan, R.A., 2008, "Sliding-mode tracking control of surface vessels," IEEE Transactions on Industrial Electronics, 55(11), 4004-4012.

[3] Bazzi, B.A. and Chalhoub, N.G., 2005, "Fuzzy-Sliding Mode Controller for a Flexible Single-Link Robotic Manipulator," Journal of Vibration and Control, 11(2), 295-314.

[4] Bennett, S., 1984, "Nicolas Minorsky and the Automatic Steering of Ships." IEEE Control Systems Magazine 4(4): 10-15.

[5] Berge, S.P., Ohtsu, K. and Fossen, T.I., 1998, "Nonlinear control of ships minimizing the position tracking errors," Proceedings of the IFAC Conference on Control Applications in Marine Systems (CAMS'98), Fukuoka, Japan, 141-147.

[6] Breivik, M., 2003, "Nonlinear maneuvering control of underactuated ships", Master Thesis, Norwegian University of Science and Technology, Trondheim, Norway.

[7] Bulian, G. (2005). "Nonlinear parametric rolling in regular waves—a general procedure for the analytical approximation of the GZ curve and its use in time domain simulations," Ocean Engineering, 32(3-4), 309-330.

[8] Caccia, M., Bibuli, M., Bono, R., Bruzzone, G., 2008 "Basic navigation, guidance and control of an Unmanned Surface Vehicle," Auton. Robot, 25, 349-365.

[9] Cammaert, A. B., & Muggeridge, D. B., 1988, "Ice interaction with offshore structures," Van Nostrand Reinhold, New York.

[10] Chalhoub, N.G., Kfoury, G.A. and Bazzi, B.A., 2006, "Design of robust controllers and a nonlinear observer for the control of a single-link flexible robotic manipulator," Journal of Sound and Vibration, 291(1-2), 437-461.

[11] Chalhoub, N.G. and Khaled N., 2014, "Integrated controller-observer system for marine surface vessels," Journal of Vibration and Control, 20(3), 381-394.

[12] Chalhoub, N.G., and Matta, S.M.A., 2012, "Robust Controller for Wheeled Mobile Robots," Proceedings of the 2012 American Control Conference (ACC), Paper FrA15.4, June 27-29, Montréal, Canada.

[13] Cheng, J., 2007, "Design of a sliding mode controller for trajectory tracking problem of marine vessels," Control Theory & Applications, IET, 1(1): 233-237.

[14] Choi, S.B. and Kim, J.S., 1997, "A Fuzzy-Sliding Mode Controller for Robust Tracking of Robotic Manipulators," Mechatronics, 7(2), 199-216.

[15] Cimen, T. and Banks, S.P., 2004, "Nonlinear optimal tracking control with application to super-tankers for autopilot design," Automatica, 40(11), 1845-1863.

[16] Clamond, D., Fructus, D., Grue, J., & Kristiansen, Ø, 2005, "An efficient model for three-dimensional surface wave simulations. Part II: Generation and absorption," Journal of Computational Physics, 205(2), 686-705.

[17] Do, K.D., Pan, J., Jiang, Z.P., 2003, "Robust adaptive control of underactuated ships on a linear course with comfort," Ocean Engineering, 30(17), 2201-2225.

[18] Drakunov, S.V., 1983, “Adaptive quasioptimal filter with discontinuous parameters,” Automation and Remote Control, 44(9), 1167-1175.

[19] Fahimi, F. and Van Kleeck, C., 2013, “Alternative trajectory-tracking control approach for marine surface vessels with experimental verification,” Robotica, 31(01), 25-33.

[20] Fossen, T.I., 1993, “High performance ship autopilot with wave filter,” Proceedings of the 10th Ship Control System Symposium (SCSS'93), Ottawa, Canada.

[21] Fossen, T.I. and Strand, J.P., 1999, “A tutorial on nonlinear backstepping: applications to ship control,” Modelling, Identification and Control, 20(2), 83-135.

[22] Fossen, T.I., 2000, “A survey on nonlinear ship control: from theory to practice,” Plenary Talk, Proceedings of the 5th IFAC Conference on Manoeuvring and Control of Marine Craft, Aalborg, Denmark.

[23] Fossen, T.I., 2002, Marine control systems: guidance, navigation and control of ships, rigs and underwater vehicles, Marine Cybernetics AS, Trondheim, ISBN 82-92356-00-2.

[24] Fossen, T.I. and Grovlen, A., 1998, “Nonlinear output feedback control of dynamically positioned ships using vectorial observer backstepping,” IEEE Transactions on Control Systems Technology, 6(1): 121-128.

[25] Fossen, T.I. and Strand, J.P., 1999, “A tutorial on nonlinear backstepping: applications to ship control,” Modelling, Identification and Control, 20(2): 83-135.

[26] Francisco, J.V., Elías, R., Eloy, L., Emiliano, M. and Haro Casado, M., 2008, "Simulations of an autonomous in-scale fast-ferry model," International Journal of Systems Applications, Engineering & Development, 2(3):114-121.

[27] Godhavn, J.M., 1996, "Nonlinear tracking of underactuated surface vessels," Proceedings of the 35th Conference Decision Control, Kobe, Japan.

[28] Godhavn, J.M., Fossen, T.I., Berge, S.P., 1998, "Nonlinear and adaptive backstepping designs for tracking control of ships," International Journal on Adaptive Control and Signal Processing (Special Issue on Marine Systems), 12, 649–670.

[29] Grace, I. F., & Ibrahim, R. A., 2008, "Modelling and analysis of ship roll oscillations interacting with stationary icebergs," Proceedings of the Institution of Mechanical Engineers, Part C: Journal of Mechanical Engineering Science, 222(10), 1873-1884.

[30] Ha, Q.P., Rye, D.C., and Durrant-Whyte, H.F., 1999, "Fuzzy Moving Sliding Mode Control With Application to Robotic Manipulators," Automatica, 35, 607-616.

[31] Hao, W., Dan, W., Peng, Z., 2013, "Adaptive dynamic surface control for cooperative path following of underactuated marine surface vehicles via fast learning," IET Control Theory and Applications, 7 (15), 1888-1898.s

[32] Healey, A.J. and Marco, D.B., 1992, "Slow speed flight control of autonomous underwater vehicles: Experimental results with the NPS AUV II," Proceedings of the 2nd International Offshore and Polar Engineering Conference (ISOPE), San Francisco, California, 523-532.

[33] Hong, G.S., 1993, "Robust control of robotic manipulators with model-based precompensation and SMC postcompensation," Journal of systems and control engineering, 207(2): 97-103.

[34] Kallstrom, C.G., Astrom, K.J., Thorell, N.E., Eriksson, J. and Sten, L., 1979, "Adaptive autopilots for tankers," Automatica, 15(3), 241-254.

[35] Kawase, K., 2012, "Concise derivation of extensive coordinate conversion formulae in the gauss-krueger projection," Geospatial Information Authority of Japan Bulletin, 60:1-6.

[36] Khaled, N. and Chalhoub, N.G., 2011, "A Dynamic Model and a Robust Controller for a Fully Actuated Marine Surface Vessel," Journal of Vibration and Control, 17(6), 801 - 812.

[37] Khaled, N., and Chalhoub, N.G., 2013, "A self-tuning guidance and control system for marine surface vessels," Nonlinear Dynamics, 73(1-2), 897–906.

[38] Khaled, N., and Chalhoub, N.G., 2014, "A self-tuning robust observer for marine surface vessels," Nonlinear Dynamics, in print.

[39] Khaled, N. and Chalhoub, N.G., 2013, "A Self-Tuning Guidance and Control System for Marine Surface Vessels," Nonlinear Dynamics, 73(1-2), 897-906.

[40] Khalil, H. K., 2002, "Nonlinear systems," Prentice Hall.

[41] Kim, M.H., 2000, Nonlinear control and robust observer design for marine vehicles, Ph.D. Dissertation, Virginia Polytechnic Institute and State University, Blacksburg, VA.

[42] Krasovskii, N. N., 1978, "Differential games. Approximation and formal models," Matematicheskii Sbornik, 149(4), 541-571.

[43] Márton, L., & Lantos, B., 2011, "Control of robotic systems with unknown friction and payload," Control Systems Technology, IEEE Transactions on, 19 (6), 1534-1539.

[44] Lauvdal, T. and Fossen, T.I., 1998, "Rudder roll stabilization of ships subject to input rate saturations using a gain scheduled control law," Proceedings of the IFAC Conference on Control Applications in Marine Systems (CAMS'98), Fukuoka, Japan, October 27-30, 121-127.

[45] Lee, H., Kim, E., Kang, H.J., Park, M., 2001, "A New Sliding-Mode Control with Fuzzy Boundary Layer," Fuzzy Sets and Systems, 120, 135-143.

[46] Lee, C.H., Newman, J.N., 1991, "First and Second Order Wave Effects on a Submerged Spheroid," Journal of Ship Research, 35 (3), 183-191.

[47] Lewandowski, E. M., 2004, "The dynamics of marine craft," Training, 2014, 11-17.

[48] Li, Z., Sun, J., Oh, S., 2009, "Design, analysis and experimental validation of a robust nonlinear path following controller for marine surface vessels," Automatica, 45, 1649-1658.

[49] Lopez, M.J., Rubio, F.R., 1992, "LQG/LTR control of ship steering autopilots," IEEE Proceedings on Intelligent Control, 447- 450.

[50] Meng, W., Guo, C., Liu, Y., 2012, "Nonlinear Sliding Mode Formation Control for Underactuated Surface Vessels," Proceedings of the 10th World Congress on Intelligent Control and Automation July 6-8, 2012, Beijing, China, 1655-1660.

[51] Minghui, W., Yongquan, Y., Yun, Z. and Fei, W., 2008, "Optimization of fuzzy control system based on extension method for ship course-changing/keeping," IEEE World Congress on Computational Intelligence, 434 – 438.

[52] Minorsky, N., 1922, "Directional stability of automatically steered bodies," Journal of the American Society of Naval Engineers, 342, 280-309.

[53] Moradi, M.H., Katebi, M.R., Johnson, M.A., 2002, "The Mimo Predictive Pid Controller Design," Asian Journal of Control, 4 (4), 452-463.

[54] Moreira, L., Fossen, T.I., and Guedes Soares, C., 2007, "Path following control system for a tanker ship model," Ocean Engineering, OE-34, 2074–2085.

[55] Nayfeh, A. H., Mook, D. T., & Marshall, L. R., 1973, Nonlinear coupling of pitch and roll modes in ship motions. Journal of Hydronautics, 7(4), 145-152.

[56] Nayfeh, A. H., & Mook, D. T. Nonlinear oscillations, 1979, John Willey and Sons, New York.

[57] Ogata, K., 1997, "Modern Control Engineering," Prentice-Hall, 3rd Edition.

[58] Ogilvie, T. F., 1974, "The Fundamental Assumptions in Ship-motion Theory," International Symposium on The Dynamics of Marine Vehicles and Structures in Waves, London, England, 148.

[59] Ogilvie, T.F., 1983, "Second-order hydrodynamic effects on ocean platforms," International Workshop on Ship and Platform Motions, University of California, Berkeley.

[60] Peng, Z., Wang, D., Chen, Z., Hu, X., Lan, W., 2013, "Adaptive Dynamic Surface Control for Formations of Autonomous Surface Vehicles With Uncertain Dynamics," IEEE Transactions on Control Systems Technology, 21 (2).

[61] Perera, L.P., Guedes Soares, C., 2012, "Pre-filtered sliding mode control for nonlinear ship steering associated with disturbances," Ocean Engineering, 51, 49-62.

[62] Perez, T., 2005, "Ship Motion Control; Course Keeping and Roll Stabilization Using Rudder and Fins," Advances in Industrial Control. Springer.

[63] Pettersen, K.Y. and Nijmeijer, H., 2001, "Underactuated ship tracking control: theory and experiments," International Journal of Control, 74(14), 1435-1446.

[64] Pivano, L., Johansen, T.A., Smogeli, O.N. and Fossen, T.I., 2007, "Nonlinear thrust controller for marine propellers in four-quadrant operations," American Control Conference, New York.

[65] Rundell, A.E., Drakunov, S.V. and DeCarlo, R.A., 1996, "A sliding mode observer and controller for stabilization of rotational motion of a vertical shaft magnetic bearing," IEEE Transactions on Control Systems Technology, 4(5), 598-608.

[66] Sagatun, S. I., 1992. "Modeling and control of underwater vehicles: A Lagrangian approach." Doctoral dissertation, The Norwegian Institute of Technology, Norway.

[67] Fossen, T. I., Sagatun, S. I., 1991, "Adaptive control of nonlinear systems: A case study of underwater robotic systems," Journal of Robotic Systems, 8(3), 393-412.

[68] Schoerling, D., Van Kleeck, C., Fahimi, F., Koch, C.R., Ams, A., and Lober, P., 2010, "Experimental test of a robust formation controller for marine unmanned surface vessels," Autonomous Robots, 28(2), 213-230.

[69] Shaocheng, T. and Li, Y, 2009, "Observer-based fuzzy adaptive control for strict-feedback nonlinear systems, Fuzzy Sets and Systems, 160(12), 1749–1764.

[70] Shaocheng, T., Changying, L., and Yongming, L., 2009, "Fuzzy adaptive observer backstepping control for MIMO nonlinear systems," Fuzzy Sets and Systems, 160(19), 2755–2775.

[71] Slotine, J.J.E., and Li, W., 1991, Applied Nonlinear Control, Englewood Cliffs, Prentice Hall, New Jersey.

[72] Strand, J.P., Ezal, K., Fossen, T.I. and Kokotovic, P.V., 1998, "Nonlinear control of ships: a locally optimal design," Reprints of the IFAC NOLCOS'98, Enschede, The Netherlands, 732-738.

[73] Suleiman, B.M., 2000, "Identification of finite-degree-of-freedom models for ship motions," Ph.D. Dissertation, Department of Engineering Mechanics, Virginia Polytechnic Institute and State University.

[74] Sun, J., Oh, S.R., 2010, "Path following of underactuated marine surface vessels using line-of-sight based model predictive control," Ocean Engineering, 37, 289-295.

[75] Utkin, V.I., 1977, "Variable structure systems with sliding-modes," IEEE Trans. Autom. Control, AC-22(2): 212–222.

[76] Utkin, V. I., 1992, "Sliding modes in control and optimization," (Vol. 116). Berlin: Springer-Verlag.

[77] Vahedipour, A., Bobis, J.P., 1992, "Smart Autopilots," Proceedings of the 1992 International Conference on Industrial Electronics, Control, Instrumentation, and Automation, Power Electronics and Motion Control., San Diego, CA, 1437-1442.

[78] Van Amerongen, J., Udink Ten Cate, A.J., 1975, "Model reference adaptive autopilots for ships," Automatica, 11(5), 441-449.

[79] Van Amerongen, J., 1984, "Adaptive steering of ships - a model reference approach," Automatica, 20 (1), 3-14.

[80] Vassalos, D., 1999, "Shaping ship safety: the face of the future," Journal of Marine Technology, 36 (2):61-74.

[81] Vassalos, D., Sarkar, T., 2000, "A RANS-based technique for simulation of the flow near a rolling cylinder at the free surface," Journal of marine science and technology, 5(2), 66-77.

[82] Vidyasagar, M., 2002, "Nonlinear systems analysis," (Vol. 42). Siam.

[83] Vukic, Z., Milinovic, D., Kuljaca, L., 1996, "Predictive gain scheduling autopilot for ships," Electrotechnical Conference MELECON '96., 8th Mediterranean (2), 1133-1136.

[84] Wang, S., 1976, "Dynamical theory of potential flows with a free surface: A classical approach to strip theory of ship motions," Journal of Ship Research, 20(3).

[85] Witkowska, A., `Smierzchalski, R., 2009, "Nonlinear backstepping ship course controller," International Journal of Automation and Computing, 6 (3), 277-284.

[86] Xu, B., 2005, "Robust nonlinear controller for underwater vehicle-manipulator systems," Proceedings of the conference on IEEE/ASME International Advanced Intelligent Mechatronics, 711-716.

[87] Zhang, X., 2010, “Chattering free SMC with robust observer and its application to inverted pendulum,” Proceedings of the 8th World Congress on Intelligent Control and Automation (WCICA), 3831-3834.

[88] Zhang, J., Feng, G., Xia, Y., 2014, “Design of Estimator-Based Sliding-Mode Output-Feedback Controllers for Discrete-Time Systems,” IEEE Transactions on Industrial Electronics, 61 (5).

ABSTRACT

EXPERIMENTAL VALIDATION OF A ROBUST SURGE SPEED CONTROLLER FOR MARINE SURFACE VESSELS

by

JOHN V. FOEHR

December 2014

Advisor: Prof. Nabil Chalhoub

Major: Mechanical Engineering

Degree: Master of Science

The focus of the current work is on providing experimental validation for the robust performance and good tracking characteristic of a surge speed controller for autonomous piloting of an under-actuated 16 ft boat in the completely uncontrolled setting of open-water Lake Saint Clair, Michigan. The controller is designed based on the sliding mode methodology and completely ignores the dynamics of the marine surface vessel (MSV) in its formulation. The testing was conducted under considerable unstructured uncertainties and unpredictable environmental disturbances induced by waves, sea-currents, and wind. The experimental results serve to validate the robust tracking characteristic of the controller and prove the successful implementation of the controller without prior knowledge of the system dynamics; thus, yielding a robust model-less controller.

AUTOBIOGRAPHICAL STATEMENT

I started out my post-high school academic career at Michigan State University without a clear major in mind. My curious personality had always been fascinated by the universe and cosmology, so I decided, despite the challenge, to endeavor to complete my Bachelors of Science degree in Astrophysics and Astronomy Research. I received my degree in 2005 after realizing a life purely devoted to academia was not for me.

After paying off my undergraduate student loans, I decided to head down a more practical career path, engineering. Upon enrolling at Wayne State University, I was required to take a handful of undergraduate level engineering courses to bridge the gap between physics and engineering. One of these courses was Dr. Chalhoub's controls engineering class and I liked the material immediately, prompting me to inquire if I could become one of his graduate students after class one day. He consented and introduced me to the boat project on which this thesis is based. After many months of coding, fabricating, installing, and testing our program on Lake St. Clair, the journey has finally concluded. Throughout all of this, Dr. Chalhoub has been a terrific mentor, who is highly concerned about his students' future and their ability to move into the engineering work force as experienced engineers, and that, is exactly what I plan to do now.